

Measurement of Dijet Azimuthal Decorrelations at Central Rapidities in $p\bar{p}$ Collisions at $\sqrt{s} = 1.96$ TeV

V. M. Abazov,³³ B. Abbott,⁷⁰ M. Abolins,⁶¹ B. S. Acharya,²⁷ D. L. Adams,⁶⁸ M. Adams,⁴⁸ T. Adams,⁴⁶ M. Agelou,¹⁷ J.-L. Agram,¹⁸ S. N. Ahmed,³² S. H. Ahn,²⁹ G. D. Alexeev,³³ G. Alkhazov,³⁷ A. Alton,⁶⁰ G. Alverson,⁵⁹ G. A. Alves,² M. Anastasoiu,³² S. Anderson,⁴² B. Andrieu,¹⁶ Y. Arnoud,¹³ A. Askew,⁷³ B. Åsman,³⁸ O. Atramentov,⁵³ C. Autermann,²⁰ C. Avila,⁷ L. Babukhadia,⁶⁷ T. C. Bacon,⁴⁰ F. Badaud,¹² A. Baden,⁵⁷ S. Baffioni,¹⁴ B. Baldin,⁴⁷ P. W. Balm,³¹ S. Banerjee,²⁷ E. Barberis,⁵⁹ P. Bargassa,⁷³ P. Baringer,⁵⁴ C. Barnes,⁴⁰ J. Barreto,² J. F. Bartlett,⁴⁷ U. Bassler,¹⁶ D. Bauer,⁵¹ A. Bean,⁵⁴ S. Beaucheron,¹⁶ F. Beaudette,¹⁵ M. Begel,⁶⁶ A. Bellavance,⁶³ S. B. Beri,²⁶ G. Bernardi,¹⁶ R. Bernhard,^{47,*} I. Bertram,³⁹ M. Besançon,¹⁷ A. Besson,¹⁸ R. Beuselinck,⁴⁰ V. A. Bezzubov,³⁶ P. C. Bhat,⁴⁷ V. Bhatnagar,²⁶ M. Bhattacharjee,⁶⁷ M. Binder,²⁴ A. Bischoff,⁴⁵ K. M. Black,⁵⁸ I. Blackler,⁴⁰ G. Blazey,⁴⁹ F. Blekman,³¹ S. Blessing,⁴⁶ D. Bloch,¹⁸ U. Blumenschein,²² A. Boehlein,⁴⁷ O. Boeriu,⁵² T. A. Bolton,⁵⁵ P. Bonamy,¹⁷ F. Borcherding,⁴⁷ G. Borissov,³⁹ K. Bos,³¹ T. Bose,⁶⁵ C. Boswell,⁴⁵ A. Brandt,⁷² G. Briskin,⁷¹ R. Brock,⁶¹ G. Brooijmans,⁶⁵ A. Bross,⁴⁷ N. J. Buchanan,⁴⁶ D. Buchholz,⁵⁰ M. Buehler,⁴⁸ V. Buescher,²² S. Burdin,⁴⁷ T. H. Burnett,⁷⁵ E. Busato,¹⁶ J. M. Butler,⁵⁸ J. Bystricky,¹⁷ F. Canelli,⁶⁶ W. Carvalho,³ B. C. K. Casey,⁷¹ D. Casey,⁶¹ N. M. Cason,⁵² H. Castilla-Valdez,³⁰ S. Chakrabarti,²⁷ D. Chakraborty,⁴⁹ K. M. Chan,⁶⁶ A. Chandra,²⁷ D. Chapin,⁷¹ F. Charles,¹⁸ E. Cheu,⁴² L. Chevalier,¹⁷ D. K. Cho,⁶⁶ S. Choi,⁴⁵ S. Chopra,⁶⁸ T. Christiansen,²⁴ L. Christofek,⁵⁴ D. Claes,⁶³ A. R. Clark,⁴³ B. Clément,¹⁸ C. Clément,³⁸ Y. Coadou,⁵ D. J. Colling,⁴⁰ L. Coney,⁵² B. Connolly,⁴⁶ M. Cooke,⁷³ W. E. Cooper,⁴⁷ D. Coppage,⁵⁴ M. Corcoran,⁷³ J. Coss,¹⁹ A. Cothenet,¹⁴ M.-C. Cousinou,¹⁴ S. Crépé-Renaudin,¹³ M. Cristetiui,⁴⁵ M. A. C. Cummings,⁴⁹ D. Cutts,⁷¹ H. da Motta,² B. Davies,³⁹ G. Davies,⁴⁰ G. A. Davis,⁵⁰ K. De,⁷² P. de Jong,³¹ S. J. de Jong,³² E. De La Cruz-Burelo,³⁰ C. De Oliveira Martins,³ S. Dean,⁴¹ K. Del Signore,⁶⁰ F. Déliot,¹⁷ P. A. Delsart,¹⁹ M. Demarteau,⁴⁷ R. Demina,⁶⁶ P. Demine,¹⁷ D. Denisov,⁴⁷ S. P. Denisov,³⁶ S. Desai,⁶⁷ H. T. Diehl,⁴⁷ M. Diesburg,⁴⁷ M. Doidge,³⁹ H. Dong,⁶⁷ S. Doulas,⁵⁹ L. Duflot,¹⁵ S. R. Dugad,²⁷ A. Duperrin,¹⁴ J. Dyer,⁶¹ A. Dyshkant,⁴⁹ M. Eads,⁴⁹ D. Edmunds,⁶¹ T. Edwards,⁴¹ J. Ellison,⁴⁵ J. Elmsheuser,²⁴ J. T. Eltzroth,⁷² V. D. Elvira,⁴⁷ S. Eno,⁵⁷ P. Ermolov,³⁵ O. V. Eroshin,³⁶ J. Estrada,⁴⁷ D. Evans,⁴⁰ H. Evans,⁶⁵ A. Evdokimov,³⁴ V. N. Evdokimov,³⁶ J. Fast,⁴⁷ S. N. Fatakia,⁵⁸ D. Fein,⁴² L. Feligioni,⁵⁸ T. Ferbel,⁶⁶ F. Fiedler,²⁴ F. Filthaut,³² W. Fisher,⁶⁴ H. E. Fisk,⁴⁷ F. Fleuret,¹⁶ M. Fortner,⁴⁹ H. Fox,²² W. Freeman,⁴⁷ S. Fu,⁴⁷ S. Fuess,⁴⁷ C. F. Galea,³² E. Gallas,⁴⁷ E. Galyaev,⁵² M. Gao,⁶⁵ C. Garcia,⁶⁶ A. Garcia-Bellido,⁷⁵ J. Gardner,⁵⁴ V. Gavrilov,³⁴ P. Gay,¹² D. Gelé,¹⁸ R. Gelhaus,⁴⁵ K. Genser,⁴⁷ C. E. Gerber,⁴⁸ Y. Gershtein,⁷¹ G. Geurkov,⁷¹ G. Ginther,⁶⁶ K. Goldmann,²⁵ T. Golling,²¹ B. Gómez,⁷ K. Gounder,⁴⁷ A. Goussiou,⁵² G. Graham,⁵⁷ P. D. Grannis,⁶⁷ S. Greder,¹⁸ J. A. Green,⁵³ H. Greenlee,⁴⁷ Z. D. Greenwood,⁵⁶ E. M. Gregores,⁴ S. Grinstein,¹ Ph. Gris,¹² J.-F. Grivaz,¹⁵ L. Groer,⁶⁵ S. Grünendahl,⁴⁷ M. W. Grünewald,²⁸ W. Gu,⁶ S. N. Gurzhiev,³⁶ G. Gutierrez,⁴⁷ P. Gutierrez,⁷⁰ A. Haas,⁶⁵ N. J. Hadley,⁵⁷ H. Haggerty,⁴⁷ S. Hagopian,⁴⁶ I. Hall,⁷⁰ R. E. Hall,⁴⁴ C. Han,⁶⁰ L. Han,⁴¹ K. Hanagaki,⁴⁷ P. Hanlet,⁷² K. Harder,⁵⁵ R. Harrington,⁵⁹ J. M. Hauptman,⁵³ R. Hauser,⁶¹ C. Hays,⁶⁵ J. Hays,⁵⁰ T. Hebbeker,²⁰ C. Hebert,⁵⁴ D. Hedin,⁴⁹ J. M. Heinmiller,⁴⁸ A. P. Heinson,⁴⁵ U. Heintz,⁵⁸ C. Hensel,⁵⁴ G. Hesketh,⁵⁹ M. D. Hildreth,⁵² R. Hirosky,⁷⁴ J. D. Hobbs,⁶⁷ B. Hoeneisen,¹¹ M. Hohlfeld,²³ S. J. Hong,²⁹ R. Hooper,⁷¹ S. Hou,⁶⁰ P. Houben,³¹ Y. Hu,⁶⁷ J. Huang,⁵¹ Y. Huang,⁶⁰ I. Iashvili,⁴⁵ R. Illingworth,⁴⁷ A. S. Ito,⁴⁷ S. Jabeen,⁵⁴ M. Jaffré,¹⁵ S. Jain,⁷⁰ V. Jain,⁶⁸ K. Jakobs,²² A. Jenkins,⁴⁰ R. Jesik,⁴⁰ Y. Jiang,⁶⁰ K. Johns,⁴² M. Johnson,⁴⁷ P. Johnson,⁴² A. Jonckheere,⁴⁷ P. Jonsson,⁴⁰ H. Jöstlein,⁴⁷ A. Juste,⁴⁷ M. M. Kado,⁴³ D. Käfer,²⁰ W. Kahl,⁵⁵ S. Kahn,⁶⁸ E. Kajfasz,¹⁴ A. M. Kalinin,³³ J. Kalk,⁶¹ D. Karmanov,³⁵ J. Kasper,⁵⁸ D. Kau,⁴⁶ Z. Ke,⁶ R. Kehoe,⁶¹ S. Kermiche,¹⁴ S. Kesisoglou,⁷¹ A. Khanov,⁶⁶ A. Kharchilava,⁵² Y. M. Kharzeev,³³ K. H. Kim,²⁹ B. Klima,⁴⁷ M. Klute,²¹ J. M. Kohli,²⁶ M. Kopal,⁷⁰ V. M. Korablev,³⁶ J. Kotcher,⁶⁸ B. Kothari,⁶⁵ A. V. Kotwal,⁶⁵ A. Koubarovsky,³⁵ O. Kouznetsov,¹³ A. V. Kozelov,³⁶ J. Kozminski,⁶¹ J. Krane,⁵³ M. R. Krishnaswamy,²⁷ S. Krzywdzinski,⁴⁷ M. Kubantsev,⁵⁵ S. Kuleshov,³⁴ Y. Kulik,⁴⁷ S. Kunori,⁵⁷ A. Kupco,¹⁷ T. Kurča,¹⁹ V. E. Kuznetsov,⁴⁵ S. Lager,³⁸ N. Lahrichi,¹⁷ G. Landsberg,⁷¹ J. Lazoflores,⁴⁶ A.-C. Le Bihan,¹⁸ P. Lebrun,¹⁹ S. W. Lee,²⁹ W. M. Lee,⁴⁶ A. Leflat,³⁵ C. Leggett,⁴³ F. Lehner,^{47,*} C. Leonidopoulos,⁶⁵ P. Lewis,⁴⁰ J. Li,⁷² Q. Z. Li,⁴⁷ X. Li,⁶ J. G. R. Lima,⁴⁹ D. Lincoln,⁴⁷ S. L. Linn,⁴⁶ J. Linnemann,⁶¹ V. V. Lipaev,³⁶ R. Lipton,⁴⁷ L. Lobo,⁴⁰ A. Lobodenko,³⁷ M. Lokajicek,¹⁰ A. Lounis,¹⁸ J. Lu,⁶ H. J. Lubatti,⁷⁵ A. Lucotte,¹³ L. Lueking,⁴⁷ C. Luo,⁵¹ M. Lynker,⁵² A. L. Lyon,⁴⁷ A. K. A. Maciel,⁴⁹ R. J. Madaras,⁴³ P. Mättig,²⁵ A. Magerkurth,⁶⁰ A.-M. Magnan,¹³ M. Maity,⁵⁸ N. Makovec,¹⁵ P. K. Mal,²⁷ S. Malik,⁵⁶ V. L. Malyshev,³³ V. Manankov,³⁵ H. S. Mao,⁶ Y. Maravin,⁴⁷ T. Marshall,⁵¹ M. Martens,⁴⁷ M. I. Martin,⁴⁹ S. E. K. Mattingly,⁷¹ A. A. Mayorov,³⁶ R. McCarthy,⁶⁷ R. McCroskey,⁴² T. McMahon,⁶⁹ D. Meder,²³ H. L. Melanson,⁴⁷ A. Melnitchouk,⁶² X. Meng,⁶ M. Merkin,³⁵ K. W. Merritt,⁴⁷ A. Meyer,²⁰ C. Miao,⁷¹

- H. Miettinen,⁷³ D. Mihalcea,⁴⁹ J. Mitrevski,⁶⁵ N. Mokhov,⁴⁷ J. Molina,³ N. K. Mondal,²⁷ H. E. Montgomery,⁴⁷ R. W. Moore,⁵ M. Mostafa,¹ G. S. Muanza,¹⁹ M. Mulders,⁴⁷ Y. D. Mutaf,⁶⁷ E. Nagy,¹⁴ F. Nang,⁴² M. Narain,⁵⁸ V. S. Narasimham,²⁷ N. A. Naumann,³² H. A. Neal,⁶⁰ J. P. Negret,⁷ S. Nelson,⁴⁶ P. Neustroev,³⁷ C. Noeding,²² A. Nomerotski,⁴⁷ S. F. Novaes,⁴ T. Nunnemann,²⁴ E. Nurse,⁴¹ V. O'Dell,⁴⁷ D. C. O'Neil,⁵ V. Oguri,³ N. Oliveira,³ B. Olivier,¹⁶ N. Oshima,⁴⁷ G. J. Otero y Garzón,⁴⁸ P. Padley,⁷³ K. Papageorgiou,⁴⁸ N. Parashar,⁵⁶ J. Park,²⁹ S. K. Park,²⁹ J. Parsons,⁶⁵ R. Partridge,⁷¹ N. Parua,⁶⁷ A. Patwa,⁶⁸ P. M. Pereira,⁴⁵ E. Perez,¹⁷ O. Peters,³¹ P. Pétreoff,¹⁵ M. Petteni,⁴⁰ L. Phaf,³¹ R. Piegaia,¹ P. L. M. Podesta-Lerma,³⁰ V. M. Podstavkov,⁴⁷ Y. Pogorelov,⁵² B. G. Pope,⁶¹ E. Popkov,⁵⁸ W. L. Prado da Silva,³ H. B. Prosper,⁴⁶ S. Protopopescu,⁶⁸ M. B. Przybycien,^{50,†} J. Qian,⁶⁰ A. Quadt,²¹ B. Quinn,⁶² K. J. Rani,²⁷ P. A. Rapidis,⁴⁷ P. N. Ratoff,³⁹ N. W. Reay,⁵⁵ J.-F. Renard,¹⁷ S. Reucroft,⁵⁹ J. Rha,⁴⁵ M. Ridel,¹⁵ M. Rijssenbeek,⁶⁷ I. Ripp-Baudot,¹⁸ F. Rizatdinova,⁵⁵ C. Royon,¹⁷ P. Rubinov,⁴⁷ R. Ruchti,⁵² B. M. Sabirov,³³ G. Sajot,¹³ A. Sánchez-Hernández,³⁰ M. P. Sanders,⁴¹ A. Santoro,³ G. Savage,⁴⁷ L. Sawyer,⁵⁶ T. Scanlon,⁴⁰ R. D. Schamberger,⁶⁷ H. Schellman,⁵⁰ P. Schieferdecker,²⁴ C. Schmitt,²⁵ A. A. Schukin,³⁶ A. Schwartzman,⁶⁴ R. Schwienhorst,⁶¹ S. Sengupta,⁴⁶ H. Severini,⁷⁰ E. Shabalina,⁴⁸ V. Shary,¹⁷ W. D. Shephard,⁵² D. Shpakov,⁵⁹ R. A. Sidwell,⁵⁵ V. Simak,⁹ V. Sirotenko,⁴⁷ D. Skow,⁴⁷ P. Skubic,⁷⁰ P. Slattery,⁶⁶ R. P. Smith,⁴⁷ K. Smolek,⁹ G. R. Snow,⁶³ J. Snow,⁶⁹ S. Snyder,⁶⁸ S. Söldner-Rembold,⁴¹ X. Song,⁴⁹ Y. Song,⁷² L. Sonnenschein,⁵⁸ A. Sopczak,³⁹ V. Sorín,¹ M. Sosebee,⁷² K. Soustruznik,⁸ M. Souza,² B. Spurlock,⁷² N. R. Stanton,⁵⁵ J. Stark,¹³ J. Steele,⁵⁶ G. Steinbrück,⁶⁵ K. Stevenson,⁵¹ V. Stolin,³⁴ A. Stone,⁴⁸ D. A. Stoyanova,³⁶ J. Strandberg,³⁸ M. A. Strang,⁷² M. Strauss,⁷⁰ R. Ströhmer,²⁴ M. Strovink,⁴³ L. Stutte,⁴⁷ S. Sumowidagdo,⁴⁶ A. Sznajder,³ M. Talby,¹⁴ P. Tamburello,⁴² W. Taylor,⁶⁷ P. Telford,⁴¹ J. Temple,⁴² S. Tentindo-Repond,⁴⁶ E. Thomas,¹⁴ B. Thooris,¹⁷ M. Tomoto,⁴⁷ T. Toole,⁵⁷ J. Torborg,⁵² S. Towers,⁶⁷ T. Trefzger,²³ S. Trincac-Duvold,¹⁶ T. G. Trippe,⁴³ B. Tuchming,¹⁷ C. Tully,⁶⁴ A. S. Turcot,⁶⁸ P. M. Tuts,⁶⁵ L. Uvarov,³⁷ S. Uvarov,³⁷ S. Uzunyan,⁴⁹ B. Vachon,⁴⁷ R. Van Kooten,⁵¹ W. M. van Leeuwen,³¹ N. Varelas,⁴⁸ E. W. Varnes,⁴² I. A. Vasilyev,³⁶ M. Vaupel,²⁵ P. Verdier,¹⁵ L. S. Vertogradov,³³ M. Verzocchi,⁵⁷ F. Villeneuve-Seguier,⁴⁰ J.-R. Vlimant,¹⁶ E. Von Toerne,⁵⁵ M. Vreeswijk,³¹ T. Vu Anh,¹⁵ H. D. Wahl,⁴⁶ R. Walker,⁴⁰ N. Wallace,⁴² Z.-M. Wang,⁶⁷ J. Warchol,⁵² M. Warsinsky,²¹ G. Watts,⁷⁵ M. Wayne,⁵² M. Weber,⁴⁷ H. Weerts,⁶¹ M. Wegner,²⁰ N. Wermes,²¹ A. White,⁷² V. White,⁴⁷ D. Whiteson,⁴³ D. Wicke,⁴⁷ D. A. Wijngaarden,³² G. W. Wilson,⁵⁴ S. J. Wimpenny,⁴⁵ J. Wittlin,⁵⁸ T. Włodek,⁷² M. Wobisch,⁴⁷ J. Womersley,⁴⁷ D. R. Wood,⁵⁹ Z. Wu,⁶ T. R. Wyatt,⁴¹ Q. Xu,⁶⁰ N. Xuan,⁵² R. Yamada,⁴⁷ M. Yan,⁵⁷ T. Yasuda,⁴⁷ Y. A. Yatsunenko,³³ Y. Yen,²⁵ K. Yip,⁶⁸ S. W. Youn,⁵⁰ J. Yu,⁷² A. Yurkewicz,⁶¹ A. Zabi,¹⁵ A. Zatserklyani,⁴⁹ M. Zdrazil,⁶⁷ C. Zeitnitz,²³ B. Zhang,⁶ D. Zhang,⁴⁷ X. Zhang,⁷⁰ T. Zhao,⁷⁵ Z. Zhao,⁶⁰ H. Zheng,⁵² B. Zhou,⁶⁰ Z. Zhou,⁵³ J. Zhu,⁵⁷ M. Zielinski,⁶⁶ D. Ziemska,⁵¹ A. Ziemska,⁵¹ R. Zitoun,⁶⁷ V. Zutshi,⁴⁹ E. G. Zverev,³⁵ and A. Zylberstejn¹⁷

(D0 Collaboration)

¹*Universidad de Buenos Aires, Buenos Aires, Argentina*²*LAFEX, Centro Brasileiro de Pesquisas Físicas, Rio de Janeiro, Brazil*³*Universidade do Estado do Rio de Janeiro, Rio de Janeiro, Brazil*⁴*Instituto de Física Teórica, Universidade Estadual Paulista, São Paulo, Brazil*⁵*University of Alberta and Simon Fraser University, Canada*⁶*Institute of High Energy Physics, Beijing, People's Republic of China*⁷*Universidad de los Andes, Bogotá, Colombia*⁸*Charles University, Center for Particle Physics, Prague, Czech Republic*⁹*Czech Technical University, Prague, Czech Republic*¹⁰*Institute of Physics, Academy of Sciences, Center for Particle Physics, Prague, Czech Republic*¹¹*Universidad San Francisco de Quito, Quito, Ecuador*¹²*Laboratoire de Physique Corpusculaire, IN2P3-CNRS, Université Blaise Pascal, Clermont-Ferrand, France*¹³*Laboratoire de Physique Subatomique et de Cosmologie, IN2P3-CNRS, Université Grenoble 1, Grenoble, France*¹⁴*CPPM, IN2P3-CNRS, Université de la Méditerranée, Marseille, France*¹⁵*Laboratoire de l'Accélérateur Linéaire, IN2P3-CNRS, Orsay, France*¹⁶*LPNHE, Universités Paris VI and VII, IN2P3-CNRS, Paris, France*¹⁷*DAPNIA/Service de Physique des Particules, CEA, Saclay, France*¹⁸*IRIS, IN2P3-CNRS, University Louis Pasteur Strasbourg, and University de Haute Alsace, France*¹⁹*Institut de Physique Nucléaire de Lyon, IN2P3-CNRS, Université Claude Bernard, Villeurbanne, France*²⁰*RWTH Aachen, III. Physikalisches Institut A, Aachen, Germany*²¹*Universität Bonn, Physikalisches Institut, Bonn, Germany*²²*Universität Freiburg, Physikalisches Institut, Freiburg, Germany*²³*Universität Mainz, Institut für Physik, Mainz, Germany*

²⁴*Ludwig-Maximilians-Universität München, München, Germany*²⁵*Fachbereich Physik, University of Wuppertal, Wuppertal, Germany*²⁶*Punjab University, Chandigarh, India*²⁷*Tata Institute of Fundamental Research, Mumbai, India*²⁸*University College Dublin, Dublin, Ireland*²⁹*Korea Detector Laboratory, Korea University, Seoul, Korea*³⁰*CINVESTAV, Mexico City, Mexico*³¹*FOM-Institute NIKHEF and University of Amsterdam/NIKHEF, Amsterdam, The Netherlands*³²*University of Nijmegen/NIKHEF, Nijmegen, The Netherlands*³³*Joint Institute for Nuclear Research, Dubna, Russia*³⁴*Institute for Theoretical and Experimental Physics, Moscow, Russia*³⁵*Moscow State University, Moscow, Russia*³⁶*Institute for High Energy Physics, Protvino, Russia*³⁷*Petersburg Nuclear Physics Institute, St. Petersburg, Russia*³⁸*Lund University, Royal Institute of Technology, Stockholm University, and Uppsala University, Sweden*³⁹*Lancaster University, Lancaster, United Kingdom*⁴⁰*Imperial College, London, United Kingdom*⁴¹*University of Manchester, Manchester, United Kingdom*⁴²*University of Arizona, Tucson, Arizona 85721, USA*⁴³*Lawrence Berkeley National Laboratory and University of California, Berkeley, California 94720, USA*⁴⁴*California State University, Fresno, California 93740, USA*⁴⁵*University of California, Riverside, California 92521, USA*⁴⁶*Florida State University, Tallahassee, Florida 32306, USA*⁴⁷*Fermi National Accelerator Laboratory, Batavia, Illinois 60510, USA*⁴⁸*University of Illinois at Chicago, Chicago, Illinois 60607, USA*⁴⁹*Northern Illinois University, DeKalb, Illinois 60115, USA*⁵⁰*Northwestern University, Evanston, Illinois 60208, USA*⁵¹*Indiana University, Bloomington, Indiana 47405, USA*⁵²*University of Notre Dame, Notre Dame, Indiana 46556, USA*⁵³*Iowa State University, Ames, Iowa 50011, USA*⁵⁴*University of Kansas, Lawrence, Kansas 66045, USA*⁵⁵*Kansas State University, Manhattan, Kansas 66506, USA*⁵⁶*Louisiana Tech University, Ruston, Louisiana 71272, USA*⁵⁷*University of Maryland, College Park, Maryland 20742, USA*⁵⁸*Boston University, Boston, Massachusetts 02215, USA*⁵⁹*Northeastern University, Boston, Massachusetts 02115, USA*⁶⁰*University of Michigan, Ann Arbor, Michigan 48109, USA*⁶¹*Michigan State University, East Lansing, Michigan 48824, USA*⁶²*University of Mississippi, University, Mississippi 38677, USA*⁶³*University of Nebraska, Lincoln, Nebraska 68588, USA*⁶⁴*Princeton University, Princeton, New Jersey 08544, USA*⁶⁵*Columbia University, New York, New York 10027, USA*⁶⁶*University of Rochester, Rochester, New York 14627, USA*⁶⁷*State University of New York, Stony Brook, New York 11794, USA*⁶⁸*Brookhaven National Laboratory, Upton, New York 11973, USA*⁶⁹*Langston University, Langston, Oklahoma 73050, USA*⁷⁰*University of Oklahoma, Norman, Oklahoma 73019, USA*⁷¹*Brown University, Providence, Rhode Island 02912, USA*⁷²*University of Texas, Arlington, Texas 76019, USA*⁷³*Rice University, Houston, Texas 77005, USA*⁷⁴*University of Virginia, Charlottesville, Virginia 22901, USA*⁷⁵*University of Washington, Seattle, Washington 98195, USA*

(Received 16 September 2004; published 7 June 2005)

Correlations in the azimuthal angle between the two largest transverse momentum jets have been measured using the D0 detector in $p\bar{p}$ collisions at a center-of-mass energy $\sqrt{s} = 1.96$ TeV. The analysis is based on an inclusive dijet event sample in the central rapidity region corresponding to an integrated luminosity of 150 pb^{-1} . Azimuthal correlations are stronger at larger transverse momenta. These are well described in perturbative QCD at next-to-leading order in the strong coupling constant, except at large azimuthal differences where contributions with low transverse momentum are significant.

Radiation of multiple quarks and gluons is one of the more complex aspects of perturbative quantum chromodynamics (PQCD), and it is being actively studied for the physics programs at the Fermilab Tevatron Collider and the CERN LHC [1]. The proper description of radiative processes is crucial for a wide range of precision measurements as well as for searches for new physical phenomena where the influence of QCD radiation is unavoidable. In this Letter we study radiative processes by examining their impact on angular distributions. We investigate the azimuthal angle between the two jets with highest transverse momenta with respect to the beam axis (p_T), $\Delta\phi_{\text{dijet}}$. Dijet production in hadron-hadron collisions, in the absence of radiative effects, results in two jets with equal transverse momenta and correlated azimuthal angles $\Delta\phi_{\text{dijet}} = \pi$. Additional radiation with low p_T causes small azimuthal decorrelations, whereas $\Delta\phi_{\text{dijet}}$ significantly lower than π is evidence of additional hard radiation with high p_T . Exclusive three-jet production populates $2\pi/3 < \Delta\phi_{\text{dijet}} < \pi$, while smaller values of $\Delta\phi_{\text{dijet}}$ require additional radiation such as a fourth jet in an event. Distributions in $\Delta\phi_{\text{dijet}}$ provide an ideal testing ground for higher-order PQCD predictions without requiring the reconstruction of additional jets and offer a way to examine the transition between soft and hard QCD processes based on a single observable.

A new measurement of azimuthal decorrelations between jets produced at high p_T in $p\bar{p}$ collisions is presented in this Letter. This is the first measurement of the differential $\Delta\phi_{\text{dijet}}$ distribution in dijet production at a hadron collider. Jets are defined using a cone algorithm [2] with radius $\mathcal{R}_{\text{cone}} = 0.7$. The same jet algorithm is used for partons in the PQCD calculations, final-state particles in the Monte Carlo event generators, and reconstructed energy depositions in the experiment. The observable, $(1/\sigma_{\text{dijet}})(d\sigma_{\text{dijet}}/d\Delta\phi_{\text{dijet}})$, is defined as the differential dijet cross section in $\Delta\phi_{\text{dijet}}$ normalized by the dijet cross section integrated over $\Delta\phi_{\text{dijet}}$ in the same phase space. (Theoretical and experimental uncertainties are reduced in this construction.) Calculations of three-jet observables at next-to-leading order (NLO) in the strong coupling constant α_s have recently become available [3,4].

Data were obtained with the D0 detector [5] in Run II of the Fermilab Tevatron Collider using $p\bar{p}$ collisions at $\sqrt{s} = 1.96$ TeV. The primary tool for jet detection was a compensating, finely segmented, liquid-argon and uranium calorimeter that provided nearly full solid-angle coverage. Calorimeter cells were grouped into projective towers focused on the nominal interaction point for trigger and reconstruction purposes. Events were acquired using multiple-stage inclusive-jet triggers. Four analysis regions were defined based on the jet with largest p_T in an event

(p_T^{\max}) with the requirement that the trigger efficiency be at least 99%. The accumulated integrated luminosities for events with $p_T^{\max} > 75, 100, 130$, and 180 GeV were $1.1, 21, 90$, and 150 pb $^{-1}$ ($\pm 6.5\%$), respectively. The second leading p_T jet in each event was required to have $p_T > 40$ GeV and both jets were required to have central rapidities with $|y_{\text{jet}}| < 0.5$ where $y_{\text{jet}} = \frac{1}{2} \ln[(E + p_z)/(E - p_z)]$ and E and p_z are the energy and the longitudinal momentum of the jet.

The position of the $p\bar{p}$ interaction was reconstructed using a tracking system consisting of silicon microstrip detectors and scintillating fibers located within a 2 T solenoidal magnet. The vertex coordinate along the beam axis was required to be within 50 cm of the detector center, which preserved the projective nature of the calorimeter towers. The systematic uncertainty associated with the vertex selection efficiency is less than 3% for $\Delta\phi_{\text{dijet}} > 2\pi/3$ and $\approx 8\%$ for $\Delta\phi_{\text{dijet}} \approx \pi/2$. The missing transverse energy was calculated from the vector sum of the individual transverse energies in calorimeter cells. Background from cosmic rays and incorrectly vertexed events was eliminated by requiring this missing transverse energy to be below $0.7p_T^{\max}$. Background introduced by electrons, photons, and detector noise that mimicked jets was eliminated based on characteristics of shower development expected for genuine jets. The overall efficiency for $\Delta\phi_{\text{dijet}} < 5\pi/6$ is 82%–84%, depending on the p_T^{\max} region. For $\Delta\phi_{\text{dijet}} \rightarrow \pi$ it drops to 76%–81%.

The p_T of each jet was corrected for calorimeter showering effects, overlaps due to multiple interactions and event pileup, calorimeter noise effects, and the energy response of the calorimeter. The calorimeter response was measured from the p_T imbalance in photon + jet events. The relative uncertainty on the jet energy calibration is $\approx 7\%$ for jets with $20 < p_T < 250$ GeV. The sensitivity of the measurement to this calibration was reduced by normalizing the $\Delta\phi_{\text{dijet}}$ distribution to the integrated dijet cross section. Nevertheless, this provides the largest contribution to the systematic uncertainty (< 7% for $\Delta\phi_{\text{dijet}} > 5\pi/6$ but up to 23% for $\Delta\phi_{\text{dijet}} < 2\pi/3$).

The correction for migrations between bins due to finite energy and position resolution was determined from events generated with the HERWIG [6] and PYTHIA [7] programs. The generated jets were smeared according to detector resolutions [8]. The angular jet resolution was determined from a full simulation of the D0 detector response. It was found to be better than 20 mrad for jets with energies above 80 GeV. The jet p_T resolution was measured from the p_T imbalance in dijet events. It decreases from 18% at $p_T = 40$ GeV to 9% for $p_T = 200$ GeV. Finite jet p_T resolution can lead to ambiguities in the selection of the two leading p_T jets. This effect is large at small $\Delta\phi_{\text{dijet}}$ where contri-

butions from higher jet multiplicities dominate. The generated events were reweighted to describe the observed $\Delta\phi_{\text{dijet}}$ distribution. This provided a good description of the observed p_T spectra of the four leading p_T jets. The correction for migrations is typically less than 8% for $\Delta\phi_{\text{dijet}} > 2\pi/3$ and $\approx 40\%$ for $\Delta\phi_{\text{dijet}} \approx \pi/2$ with a model dependence of less than 2%. Only for $p_T^{\max} < 130 \text{ GeV}$ and at $\Delta\phi_{\text{dijet}} \approx \pi/2$ is the model dependence as large as $\approx 14\%$. The model dependence was taken into account in the evaluation of the overall systematic uncertainty.

The corrected data are presented in Fig. 1 as a function of $\Delta\phi_{\text{dijet}}$ in four ranges of p_T^{\max} . The inner error bars represent the statistical uncertainties, and the outer error bars correspond to the quadratic sum of the statistical and systematic uncertainties. The systematic uncertainties include contributions from the sources described above: event selection efficiency, jet energy calibration, and the model dependence in the correction for migrations. The spectra are strongly peaked at $\Delta\phi_{\text{dijet}} \approx \pi$; the peaks are narrower at larger values of p_T^{\max} . Overlaid on the data points in Fig. 1 are the results of PQCD calculations obtained using the parton-level event generator NLOJET++ [4]

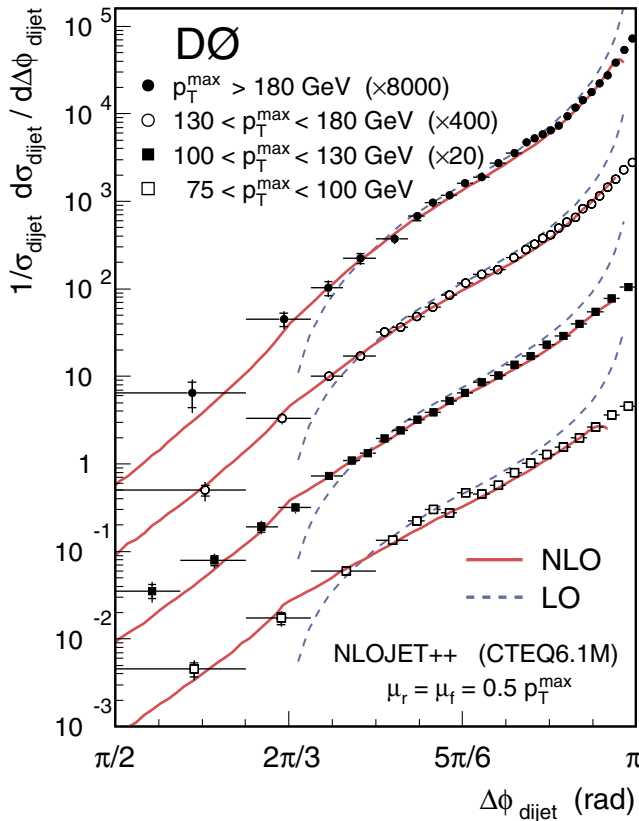


FIG. 1 (color online). The $\Delta\phi_{\text{dijet}}$ distributions in four regions of p_T^{\max} . Data and predictions with $p_T^{\max} > 100 \text{ GeV}$ are scaled by successive factors of 20 for purposes of presentation. The solid (dashed) lines show the NLO (LO) PQCD predictions.

and CTEQ6.1M [9] parton distribution functions (PDFs) with $\alpha_s(M_Z) = 0.118$. The leading order (LO) PQCD prediction for the observable was calculated from the ratio of the predictions for $2 \rightarrow 3$ processes ($d\sigma_{\text{dijet}}/d\Delta\phi_{\text{dijet}}$) and $2 \rightarrow 2$ processes (σ_{dijet}), both at LO. The NLO prediction of the observable was analogously obtained from the NLO results of the individual pieces,

$$\frac{1}{\sigma_{\text{dijet}}} \left|_{(N)\text{LO}} \right. \frac{d\sigma_{\text{dijet}}}{d\Delta\phi_{\text{dijet}}} \left|_{(N)\text{LO}} \right..$$

The renormalization and factorization scales are chosen to be $\mu_r = \mu_f = 0.5 p_T^{\max}$. The ratio is insensitive to hadronization corrections and the underlying event [10].

As shown in Fig. 2, data and NLO agree within 5%–20%. The theoretical uncertainty due to the PDFs [9] is estimated to be below 20%. Also shown is the effect of renormalization and factorization scale variation ($0.25 p_T^{\max} < \mu_{r,f} < p_T^{\max}$). The large scale dependence for $\Delta\phi_{\text{dijet}} < 2\pi/3$ occurs because the NLO calculation receives contributions only from tree-level four-parton final states in this regime. Results from PQCD at large

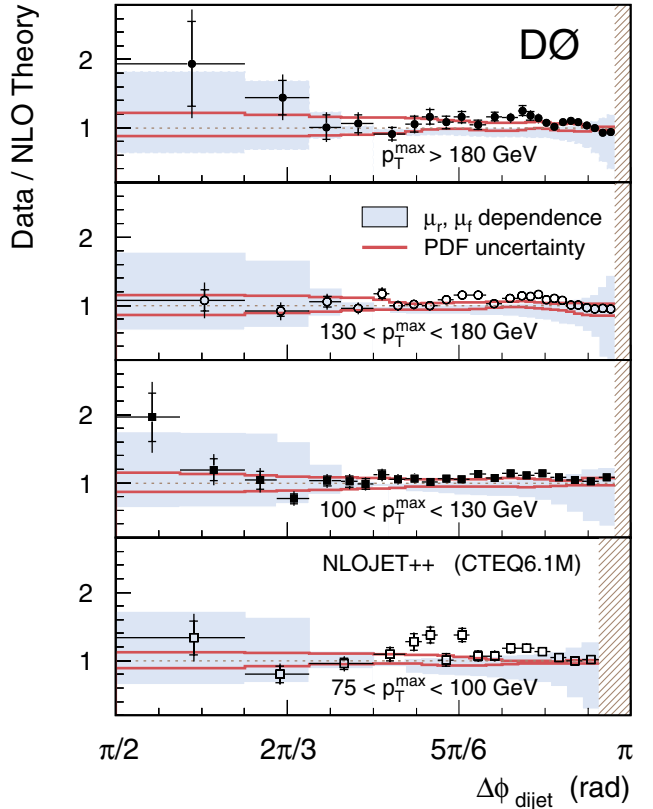


FIG. 2 (color online). Ratios of data to the NLO PQCD calculation for different regions of p_T^{\max} . Theoretical uncertainties due to variation of μ_r and μ_f are shown as the shaded regions; the uncertainty due to the PDFs is indicated by the solid lines. The points at large $\Delta\phi_{\text{dijet}}$ are excluded because the calculation is not stable near the divergence at π .

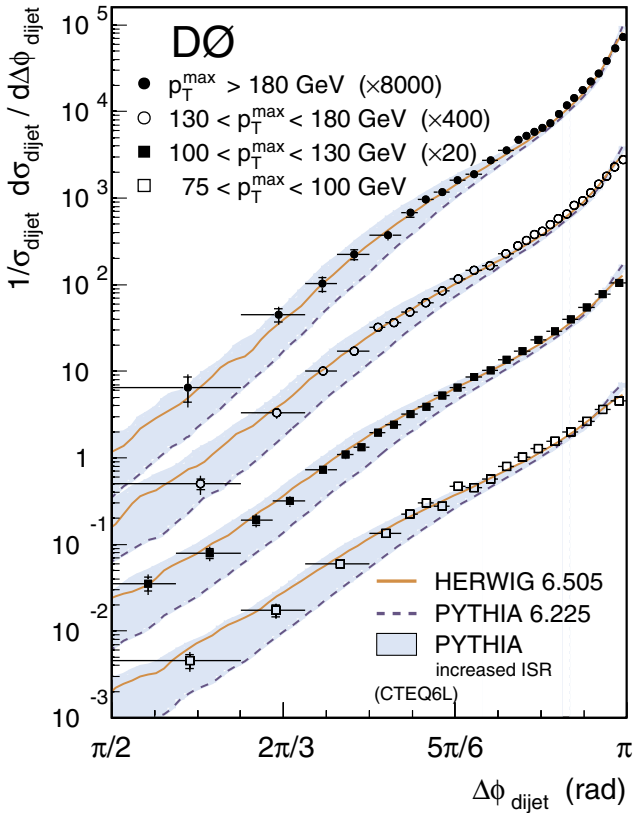


FIG. 3 (color online). The $\Delta\phi_{\text{dijet}}$ distributions in different p_T^{max} ranges. Results from HERWIG and PYTHIA are overlaid on the data. Data and predictions with $p_T^{\text{max}} > 100$ GeV are scaled by successive factors of 20 for purposes of presentation.

$\Delta\phi_{\text{dijet}}$ in Figs. 1 and 2 were excluded because fixed-order perturbation theory fails to describe the data in the region $\Delta\phi_{\text{dijet}} \approx \pi$ where soft processes dominate. Overall, NLO PQCD provides a good description of the data although differences in shape can be discerned for $\Delta\phi_{\text{dijet}} \gtrsim 5\pi/6$. In this region, the observable probes the transition between two- and three-jet configurations. The cone algorithm is sensitive to the fine details of the event topology in this transition region. These details may not be adequately described by low-order PQCD, and higher-order calculations may be required.

Monte Carlo event generators, such as HERWIG and PYTHIA, use $2 \rightarrow 2$ LO PQCD matrix elements with phenomenological parton-shower models to simulate higher-order QCD effects. Results from HERWIG (version 6.505) and PYTHIA (version 6.225), both using default parameters and the CTEQ6L [9] PDFs, are compared to the data in Fig. 3. HERWIG describes the data well over the entire $\Delta\phi_{\text{dijet}}$ range including $\Delta\phi_{\text{dijet}} \approx \pi$. PYTHIA with default parameters describes the data poorly—the distribution is too narrowly peaked at $\Delta\phi_{\text{dijet}} \approx \pi$ and lies significantly below the data over most of the $\Delta\phi_{\text{dijet}}$ range. The maximum p_T^2 in the initial-state parton shower is directly related

to the maximum virtuality that can be adjusted in PYTHIA. The shaded bands in Fig. 3 indicate the range of variation when the maximum allowed virtuality is smoothly increased from the current default by a factor of 4 [11]. These variations result in significant changes in the low $\Delta\phi_{\text{dijet}}$ region clearly demonstrating the sensitivity of this measurement. Consequently, global efforts to tune Monte Carlo event generators should benefit from including our data.

To summarize, we have measured the dijet azimuthal decorrelation in different ranges of leading jet p_T and observe an increased decorrelation towards smaller p_T . NLO PQCD describes the data except for very large $\Delta\phi_{\text{dijet}}$ where the calculation is not predictive.

We thank W. Giele, Z. Nagy, M. H. Seymour, and T. Sjöstrand for many helpful discussions. We thank the staffs at Fermilab and collaborating institutions, and acknowledge support from the Department of Energy and National Science Foundation (USA), Commissariat à l'Energie Atomique and CNRS/Institut National de Physique Nucléaire et de Physique des Particules (France), Ministry of Education and Science, Agency for Atomic Energy and RF President Grants Program (Russia), CAPES, CNPq, FAPERJ, FAPESP, and FUNDUNESP (Brazil), Departments of Atomic Energy and Science and Technology (India), Colciencias (Colombia), CONACyT (Mexico), KRF (Korea), CONICET and UBACyT (Argentina), The Foundation for Fundamental Research on Matter (The Netherlands), PPARC (United Kingdom), Ministry of Education (Czech Republic), Natural Sciences and Engineering Research Council and WestGrid Project (Canada), BMBF and DFG (Germany), A. P. Sloan Foundation, Civilian Research and Development Foundation, Research Corporation, Texas Advanced Research Program, and the Alexander von Humboldt Foundation.

*Visitor from University of Zurich, Zurich, Switzerland.

[†]Visitor from Institute of Nuclear Physics, Krakow, Poland.

- [1] M. Dobbs *et al.*, hep-ph/0403100.
- [2] We are using the iterative, seed-based cone algorithm including midpoints, as described on p. 47, Sect. 3.5 in G. C. Blazey *et al.*, in *Proceedings of the Workshop: QCD and Weak Boson Physics in Run II*, edited by U. Baur, R. K. Ellis, and D. Zeppenfeld (Fermilab, Batavia, IL, 2000).
- [3] W. B. Kilgore and W. T. Giele, in *Proceedings of the 35th Rencontres De Moriond, Les Arcs, France, 2000*, edited by J. Tran Thanh Van (EDP Sciences, Les Ulis, France, 2001).
- [4] Z. Nagy, Phys. Rev. Lett. **88**, 122003 (2002); Z. Nagy, Phys. Rev. D **68**, 094002 (2003).
- [5] D0 Collaboration, V. Abazov *et al.*, Nucl. Instrum. Methods Phys. Res., Sect. A (to be published); T. LeCompte and H. T. Diehl, Annu. Rev. Nucl. Part. Sci.

- 50**, 71 (2000); D0 Collaboration, S. Abachi *et al.*, Nucl. Instrum. Methods Phys. Res., Sect. A **338**, 185 (1994).
- [6] G. Marchesini *et al.*, Comput. Phys. Commun. **67**, 465 (1992); G. Corcella *et al.*, J. High Energy Phys. 01 (2001) 010.
- [7] T. Sjöstrand *et al.*, Comput. Phys. Commun. **135**, 238 (2001).
- [8] A. Kupčo, Ph.D. thesis, Charles University, Prague, Czech Republic, 2003 (unpublished).
- [9] J. Pumplin *et al.*, J. High Energy Phys. 07 (2002) 12; D. Stump *et al.*, J. High Energy Phys. 10 (2003) 046.
- [10] M. Wobisch, hep-ex/0411025 (to be published).
- [11] The PYTHIA parameter PARP(67) was increased from the current default of 1.0 to 4.0 which was the default before version 6.138. A variation in this range is generally considered to be reasonable [12]. The maximum virtuality in the initial-state parton shower is defined by the product of PARP(67) and the square of the hard-scattering scale.
- [12] T. Sjöstrand, L. Lönnblad, and S. Mrenna, PYTHIA 6.2 Physics and Manual, LU-TP 01-21 (2001), hep-ph/0108264.